Appendix A   Comparison between Present and STAGS Results

In this appendix the displacement, strain, and stress resultant responses are shown for eight and nine layer graphite-epoxy cylinders with semi-major diameters of 5 in., ellipticities of 0.7, and lengths of 12.5 in. These responses are computed with the semi-analytical solution of the present study and with the finite element code STAGS [A-1]. Only geometrically nonlinear analyses are considered. The material and geometric properties of a layer of graphite-epoxy are taken to be

$$\begin{array}{ccc} E_1 = 18.85 \ \text{Msi} & E_2 = 1.407 \ \text{Msi} & \\ G_{12} = 0.725 \ \text{Msi} & \nu_{12} = 0.300 & h = 0.0055 \ \text{in.} \end{array} \tag{A.1}$$

where h is the thickness of a single layer. The laminates considered are: quasi-isotropic, $[\pm45/0/90]_S$; axially-stiff, $[\pm45/0_2/90_{1/2}]_S$; circumferentially-stiff, $[\pm45/90_2/0_{1/2}]_S$, where 0 degrees is in the axial direction.

The mesh for the semi-analytical solution has 125 finite-difference nodes in the axial direction and 100 nodes around the circumference for a total of 12,500 nodes. In the axial direction the distance between nodes is adjusted by the finite-difference scheme according to the magnitude of the axial gradients in the response quantities. In the circumferential direction the distance between nodes is 0.2718 in. The STAGS mesh has 41 nodes in the axial direction and 97 nodes around the circumference, for a total of 3997 nodes and 3840 elements. The nodes are equispaced in both directions and the length of the element is 0.3125 in. in the axial direction and 0.2803 in. in the circumferential direction. Essentially, the mesh is finer in the present solution than for the STAGS solution. The difference in the mesh between the present and STAGS solution is most significant in the axial direction, as is apparent in figs. A-1 - A-18.

For the STAGS solution the displacements are computed at the nodes. The strains, curvatures, force resultants, moment resultants, and shear force resultants are computed at the Gauss points, which are located at the center of the element. Therefore, for the STAGS solutions there are no results for the ends of the cylinder, which is where failure is predicted to occur. By increasing the number of points in the axial direction, the Gauss points can approach the ends of the cylinder, but they can never reach the ends. For this reason, a failure prediction using STAGS results will not agree with a failure prediction using the present analysis. For a given failure criterion, STAGS will be nonconservative.

References

A-1. Brogan, F.A., Rankin, C.C., and Cabiness, H.D., "STAGS Users Manual," Lockheed Palo Alto Research Laboratory Report LMSC PO32594, 1994.

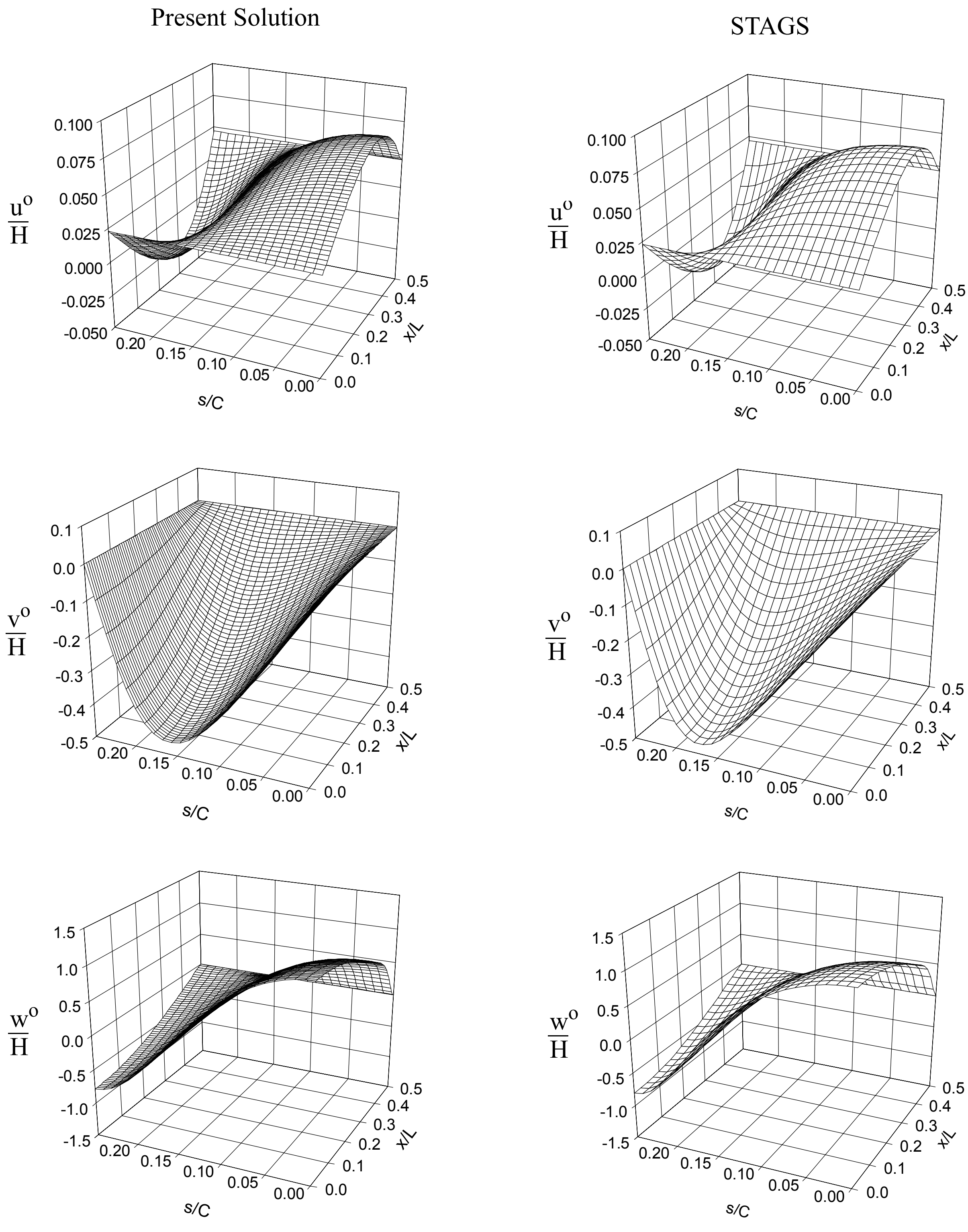

Figure A-1 Comparison between present solution and STAGS for a quasi-isotropic elliptical cylinder, e=0.7, p_o=100 psi: displacements

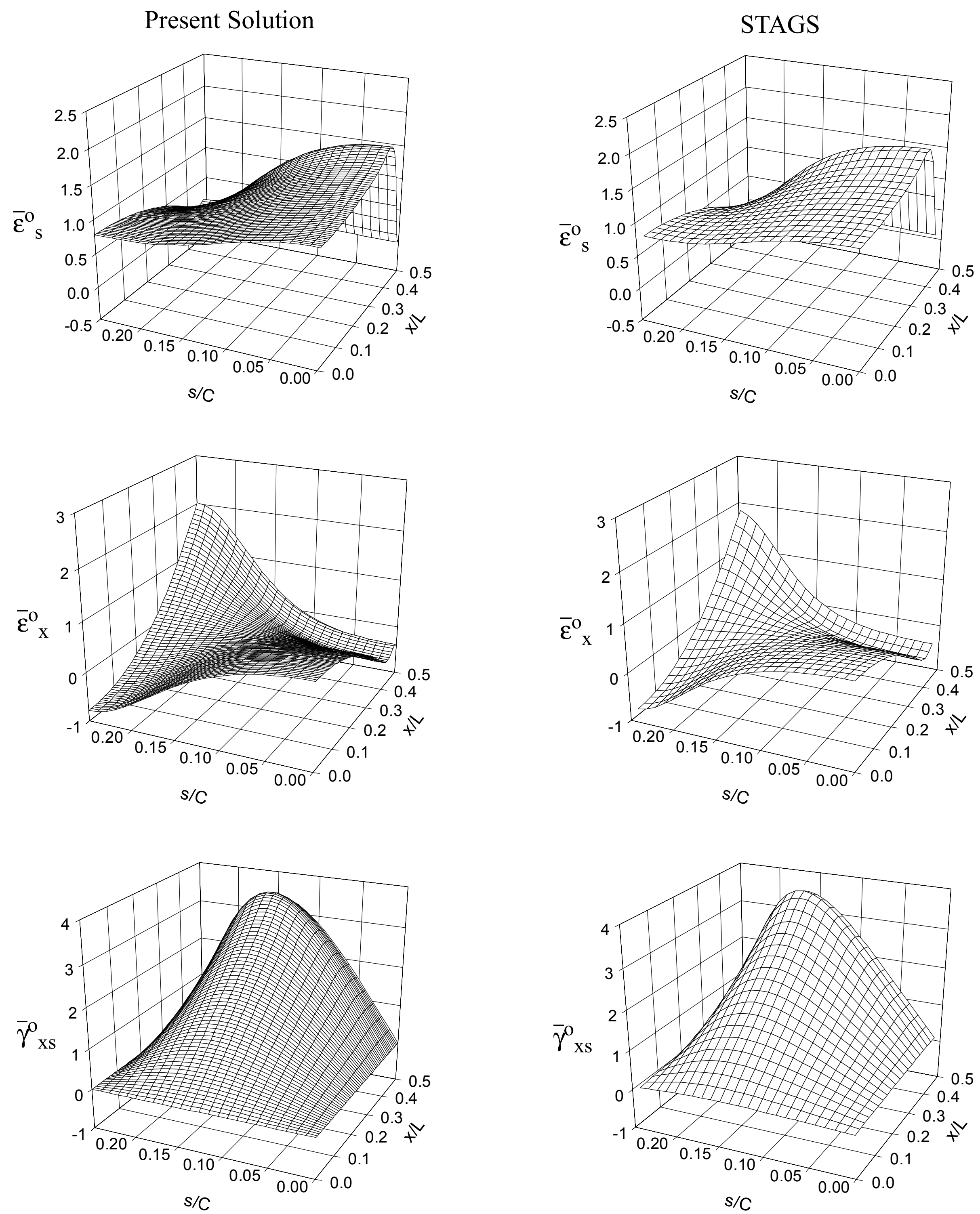

Figure A-2 Comparison between present solution and STAGS for a quasi-isotropic elliptical cylinder, e=0.7, p_o=100 psi: reference surface strains

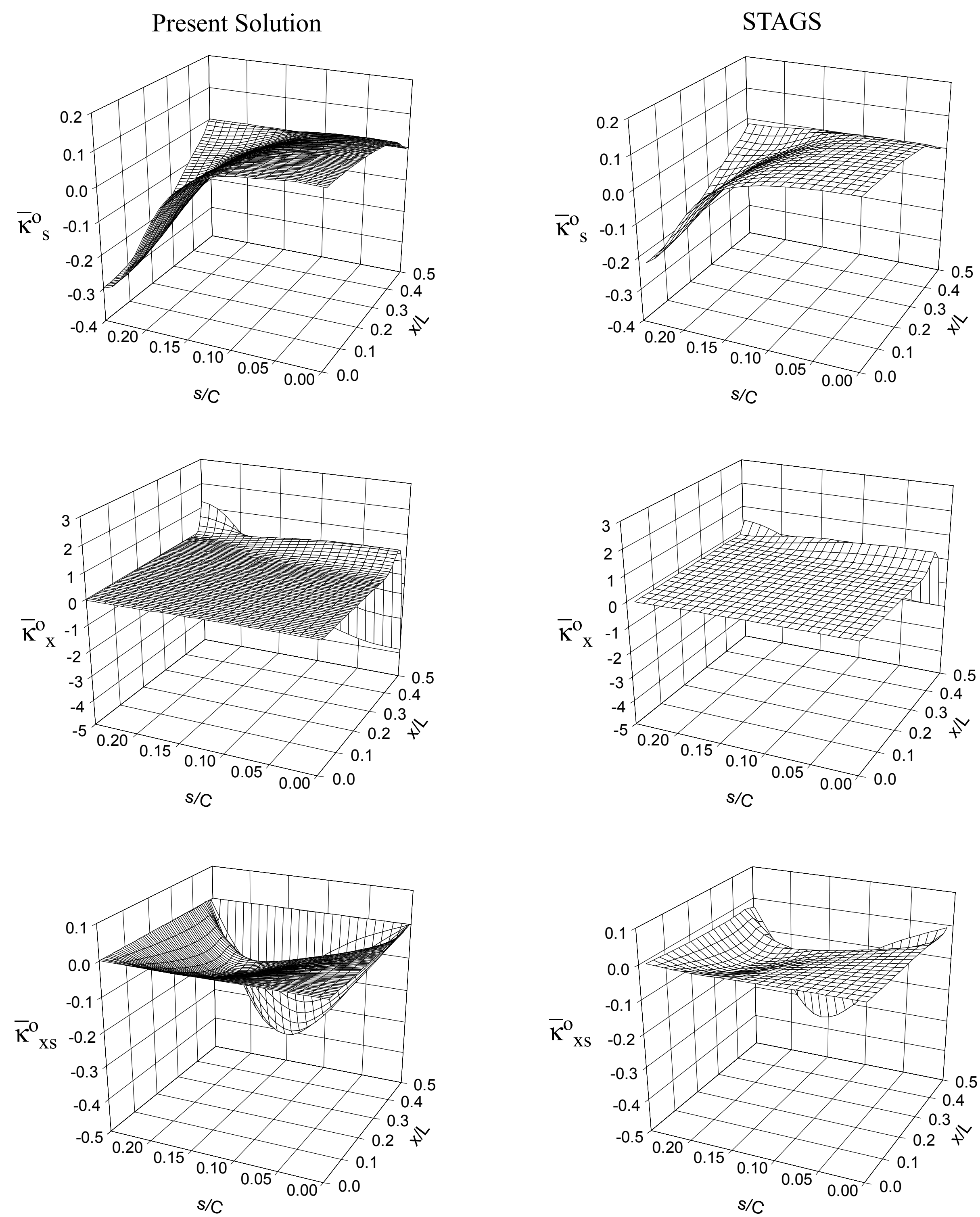

Figure A-3 Comparison between present solution and STAGS for a quasi-isotropic elliptical cylinder, e=0.7, p_o=100 psi: reference surface curvatures

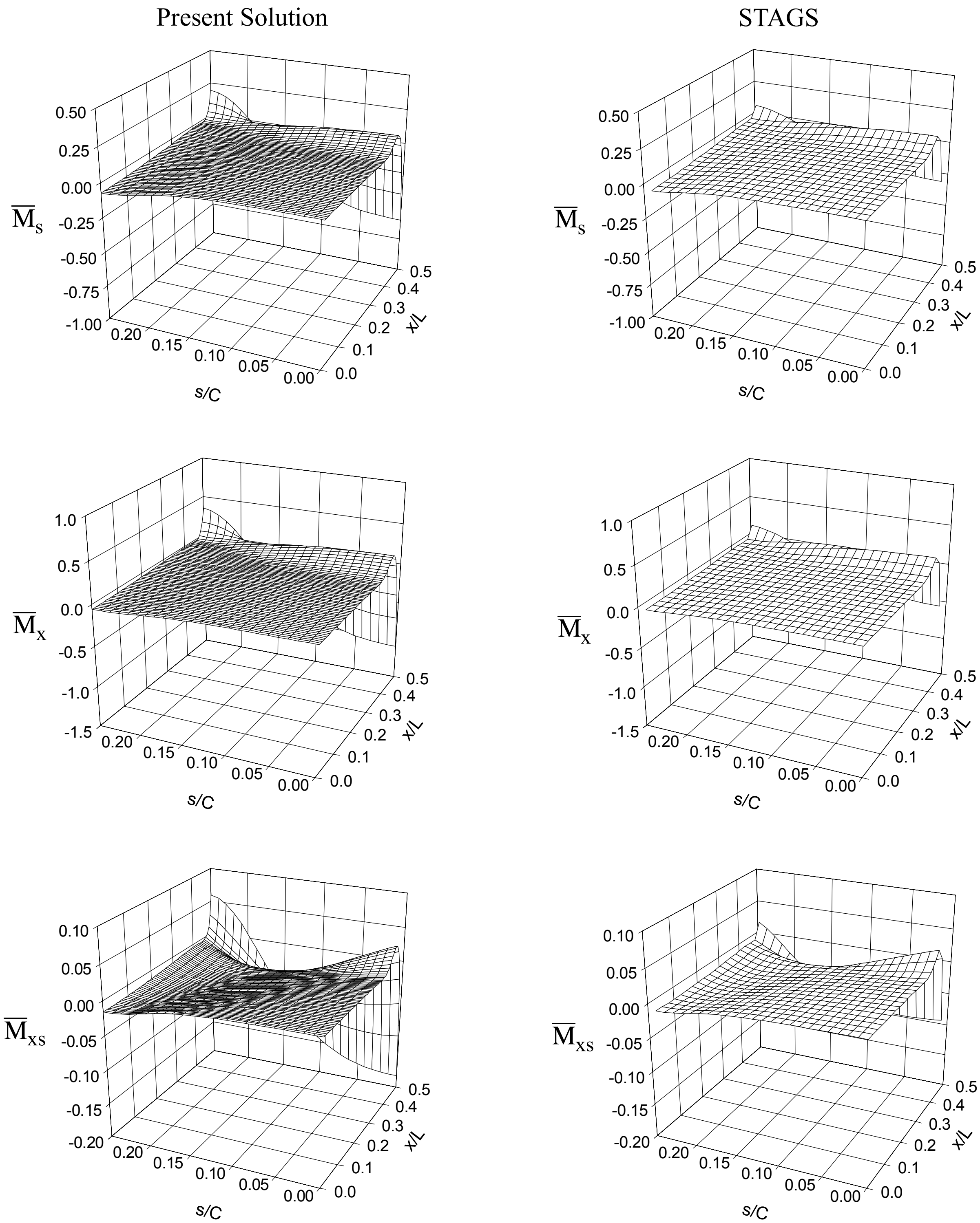

Figure A-4 Comparison between present solution and STAGS for a quasi-isotropic elliptical cylinder, e=0.7, p_o=100 psi: moment resultants

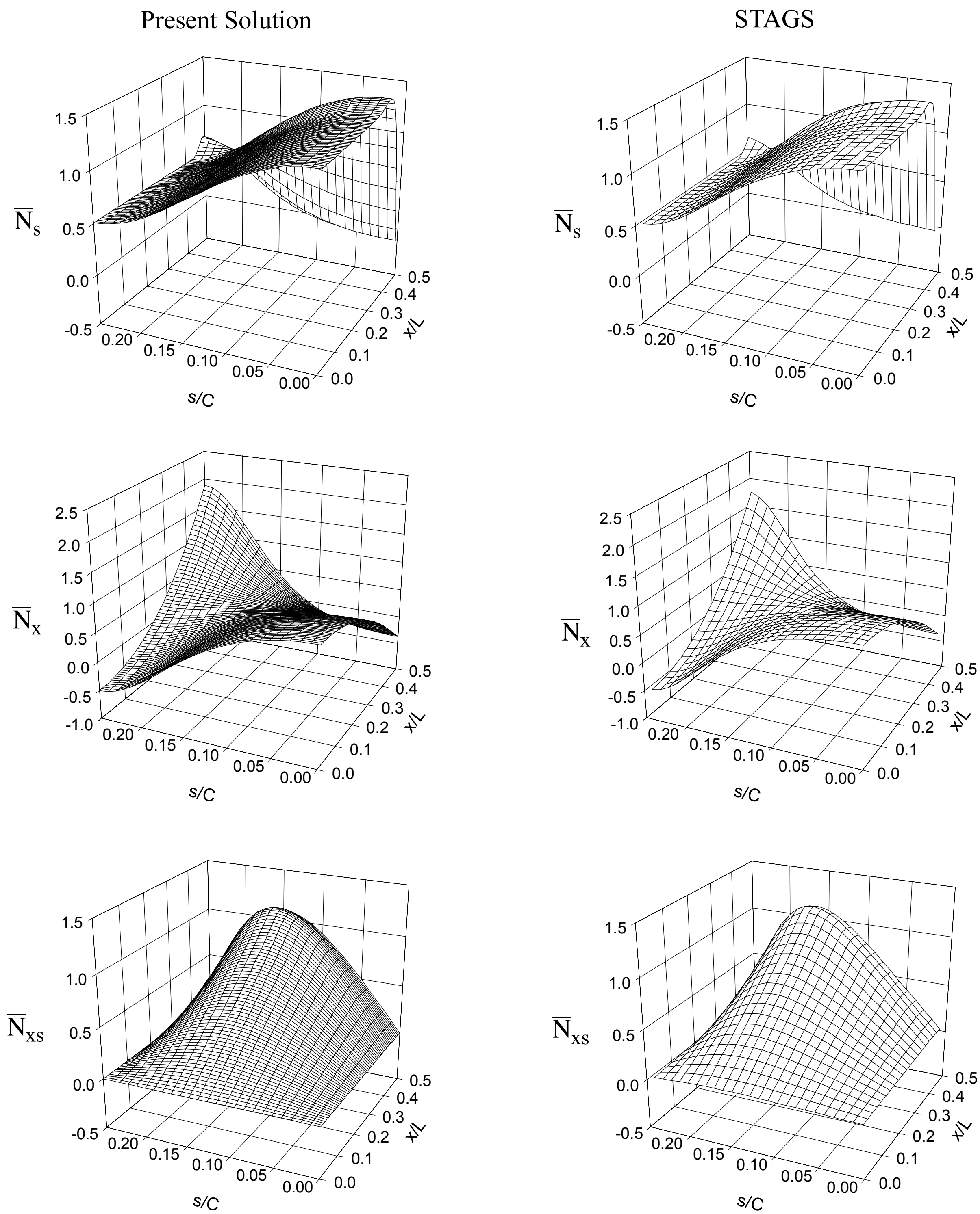

Figure A-5 Comparison between present solution and STAGS for a quasi-isotropic elliptical cylinder, e=0.7, p_o=100 psi: force resultants

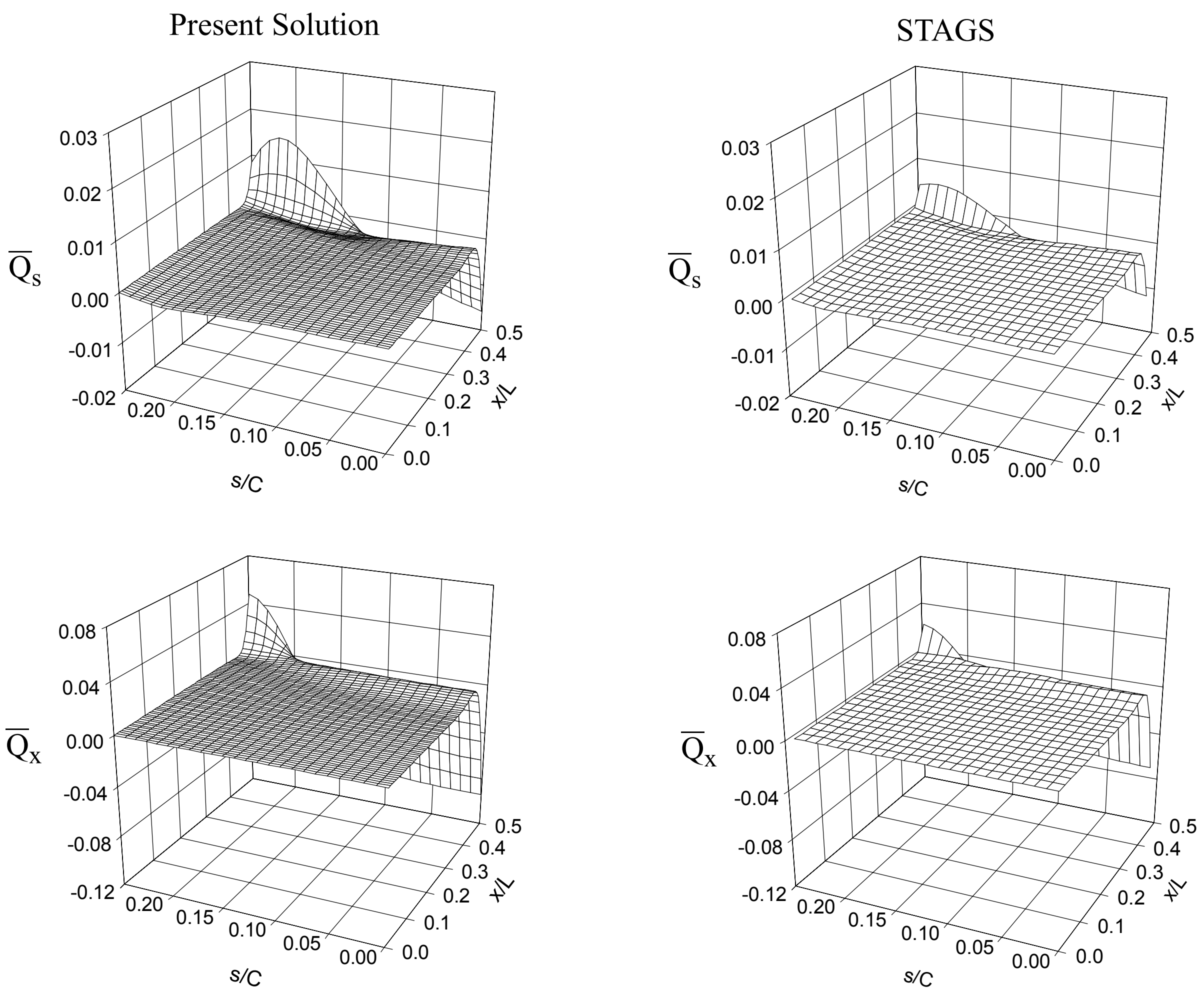

Figure A-6 Comparison between present solution and STAGS for a quasi-isotropic elliptical cylinder, e=0.7, p_o=100 psi: transverse shear force resultants

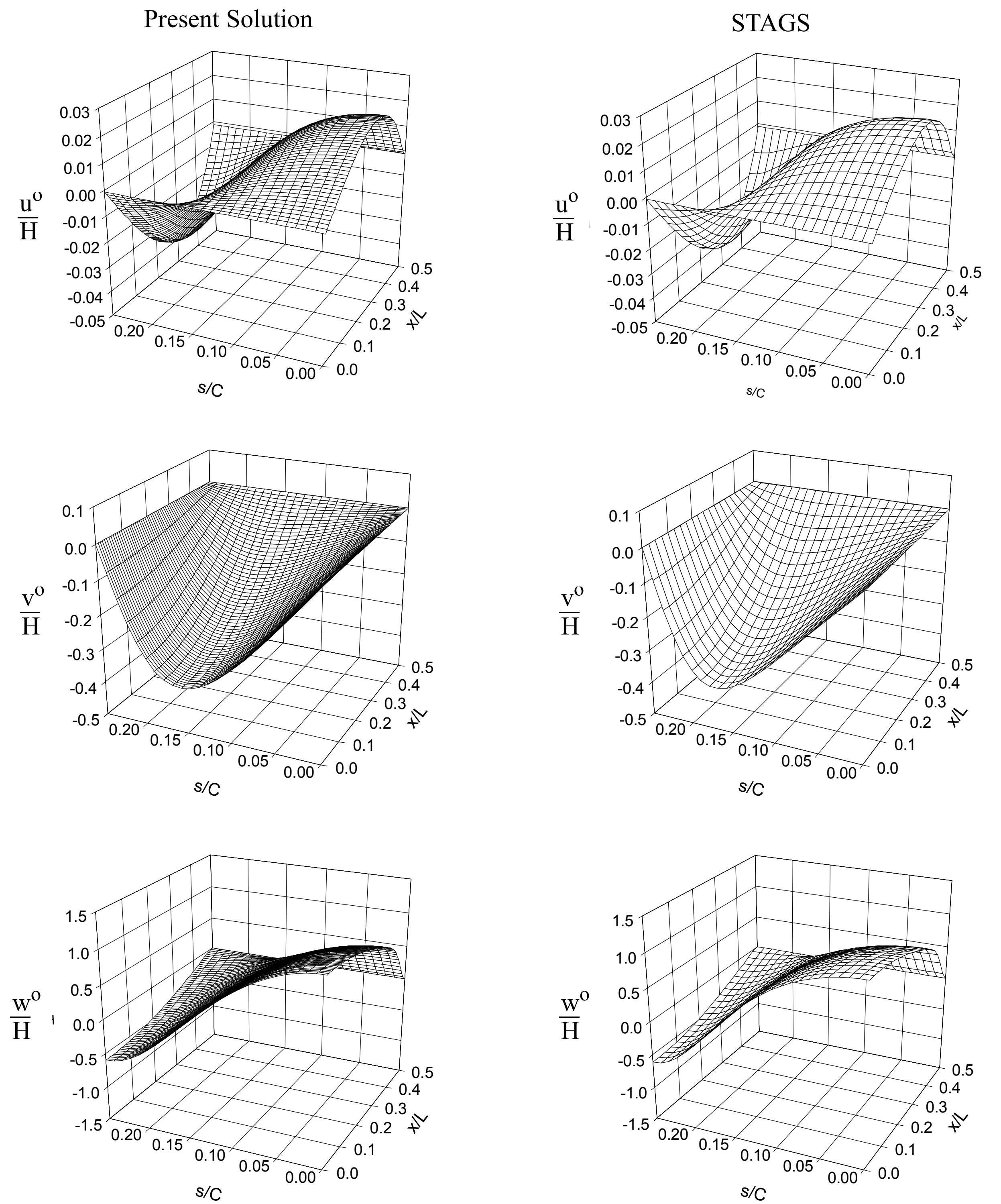

Figure A-7 Comparison between present solution and STAGS for an axially-stiff elliptical cylinder, e=0.7, p_o=100 psi: displacements

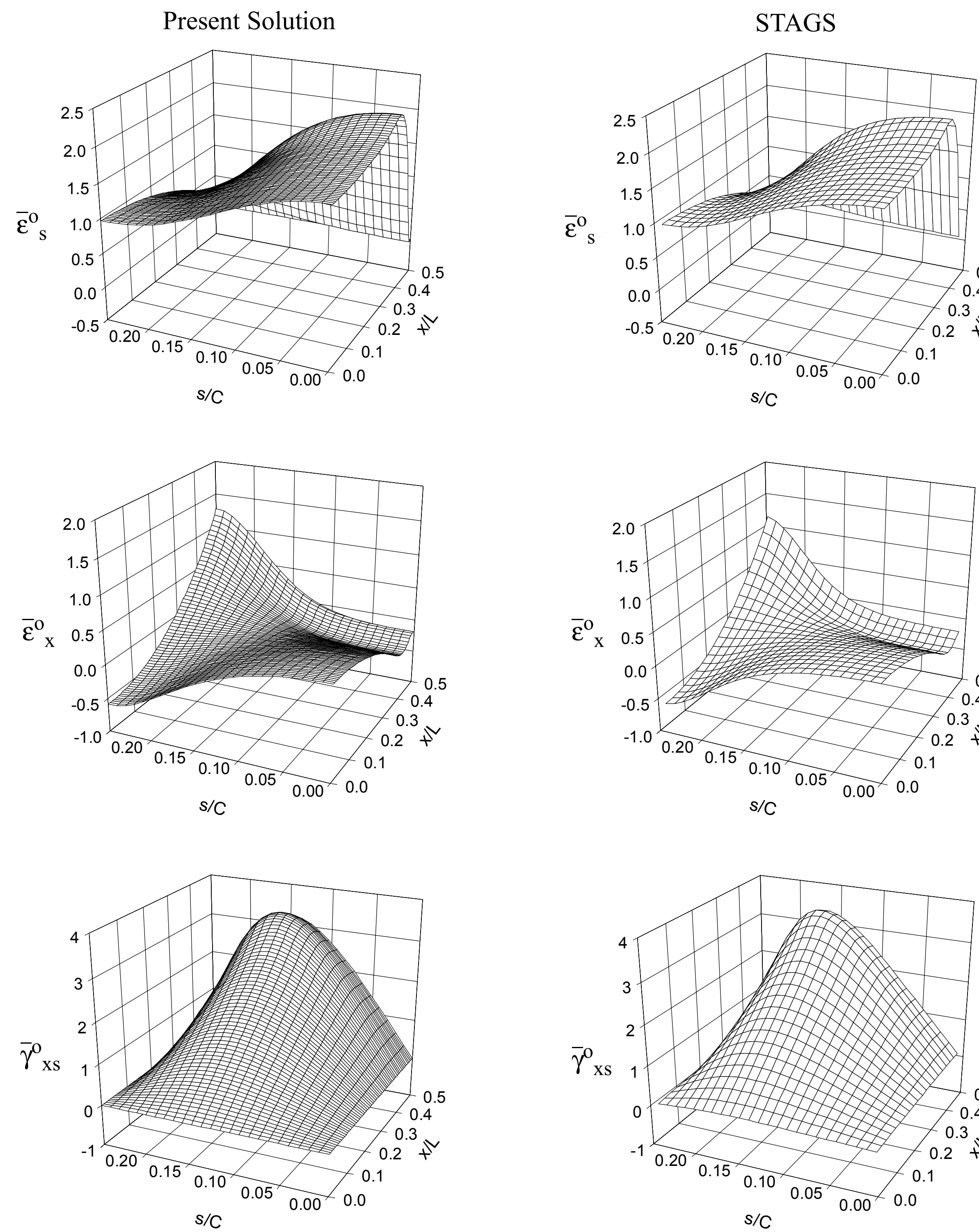

Figure A-8 Comparison between present solution and STAGS for an axially-stiff elliptical cylinder, e=0.7, p_o=100 psi: reference surface strains

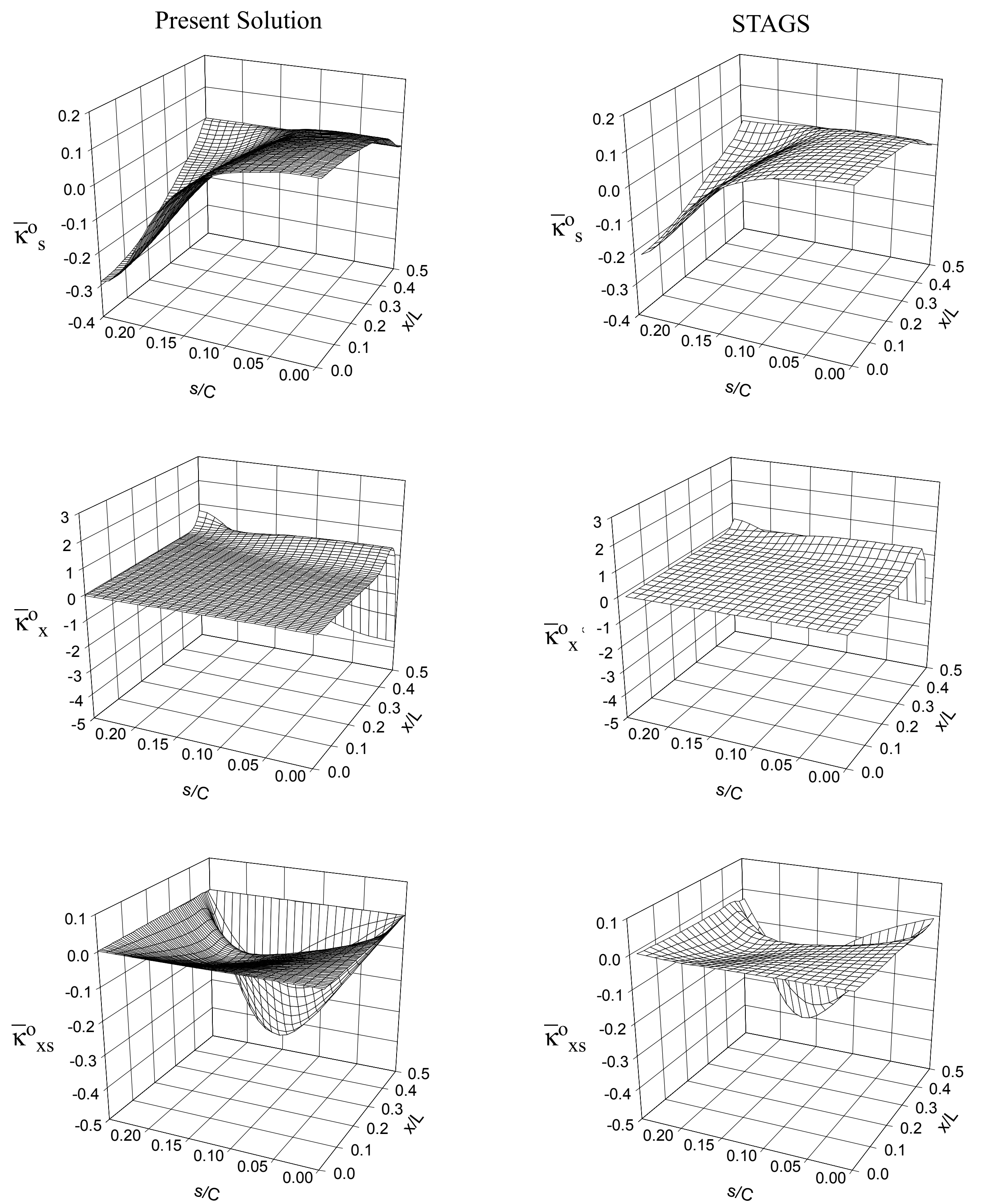

Figure A-9 Comparison between present solution and STAGS for an axially-stiff elliptical cylinder, e=0.7, p_o=100 psi: reference surface curvatures

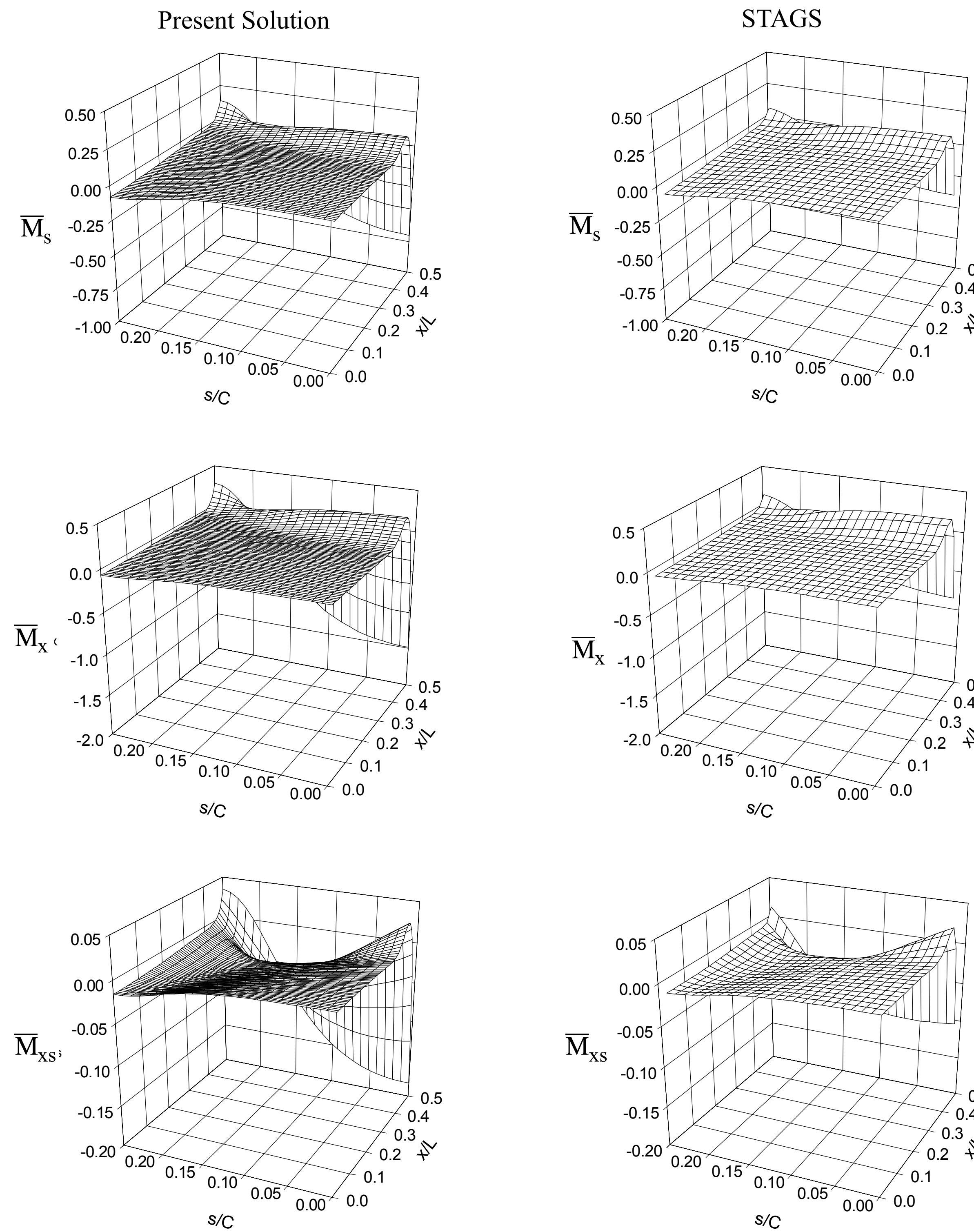

Figure A-10 Comparison between present solution and STAGS for an axially-stiff elliptical cylinder, e=0.7, p_o=100 psi: moment resultants

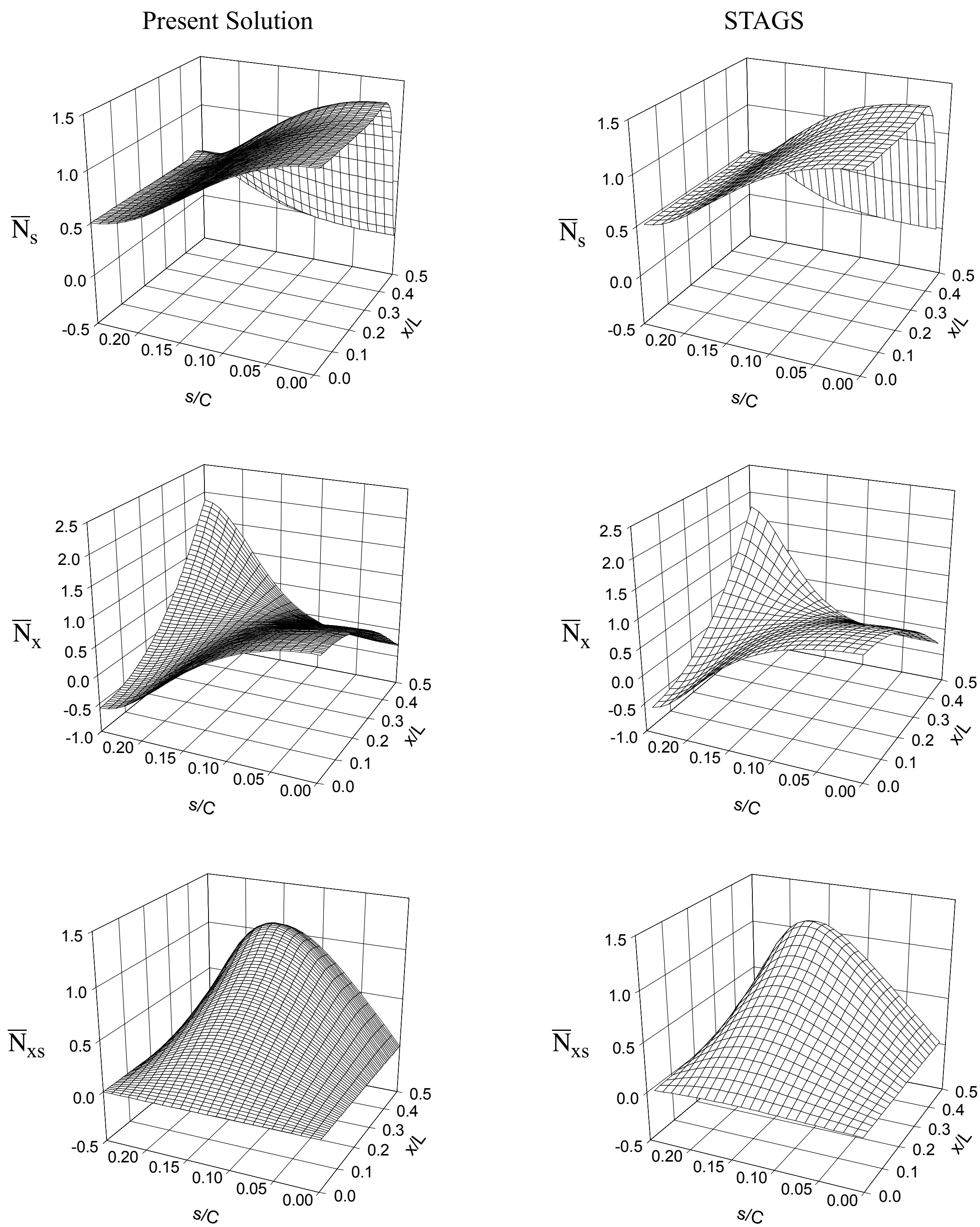

Figure A-11 Comparison between present solution and STAGS for an axially-stiff elliptical cylinder, e=0.7, p_o=100 psi: force resultants

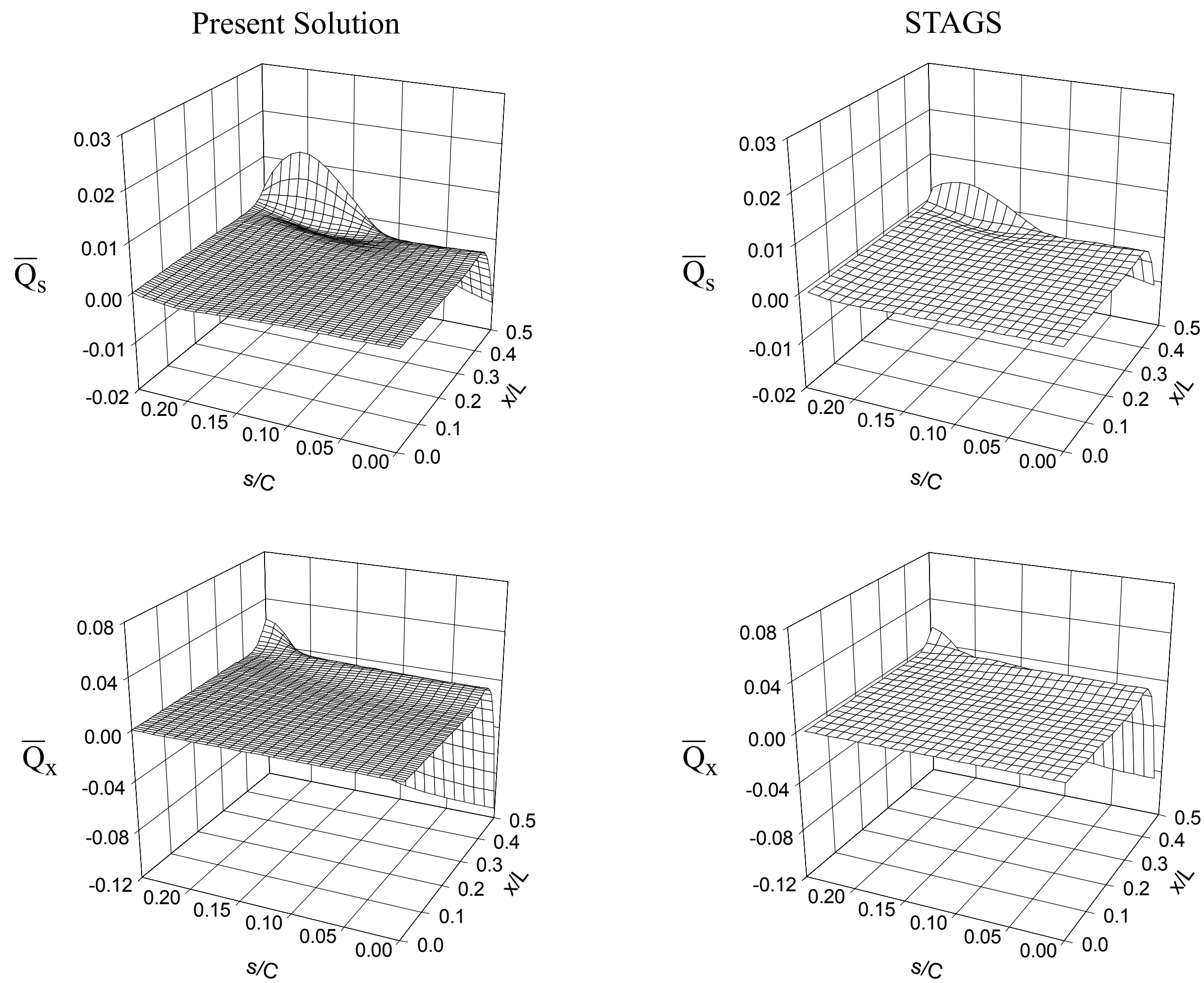

Figure A-12 Comparison between present solution and STAGS for an axially-stiff elliptical cylinder, e=0.7, p_o=100 psi: transverse shear force resultants

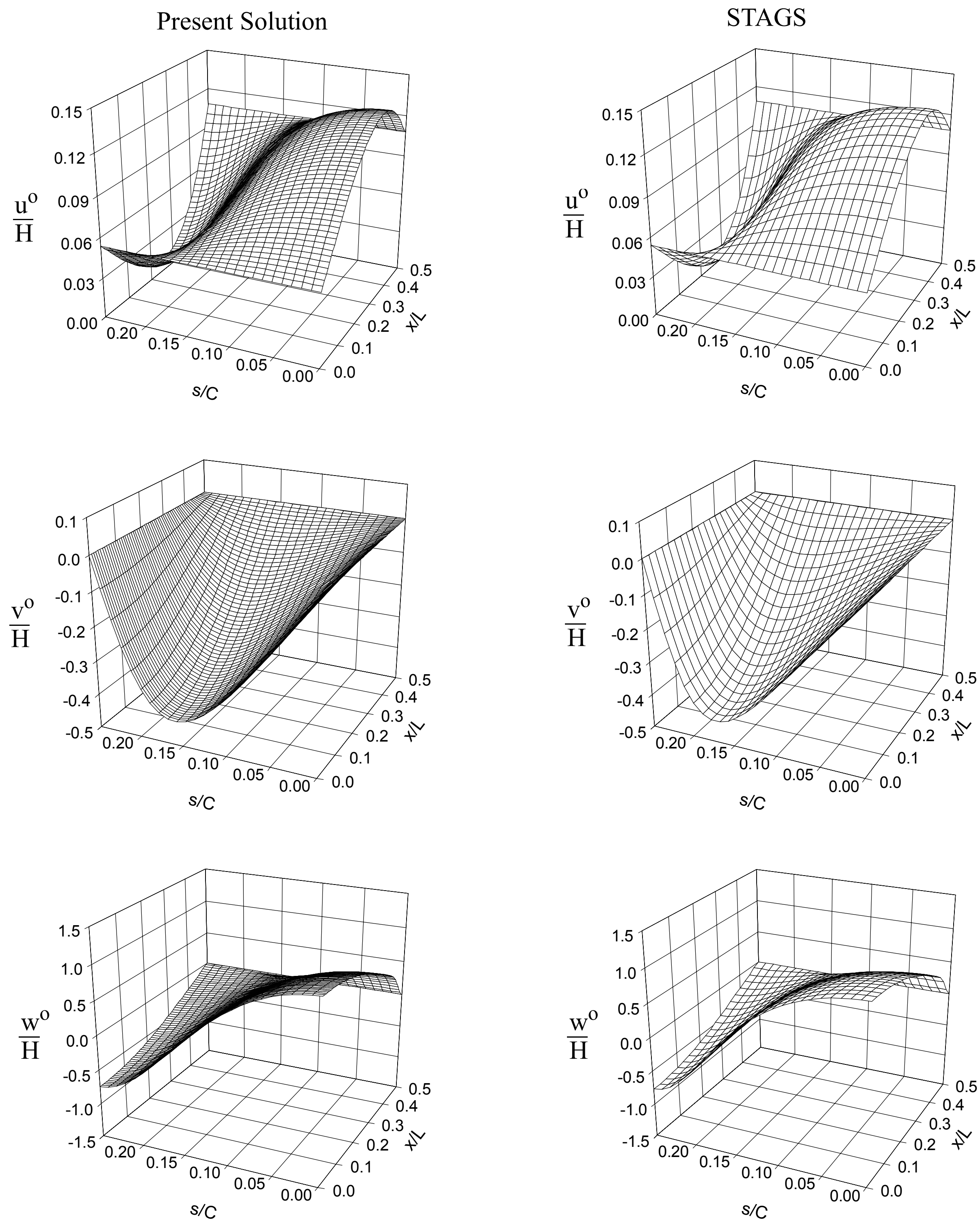

Figure A-13 Comparison between present solution and STAGS for an circumferentially-stiff elliptical cylinder, e=0.7, p_o=100 psi: displacements

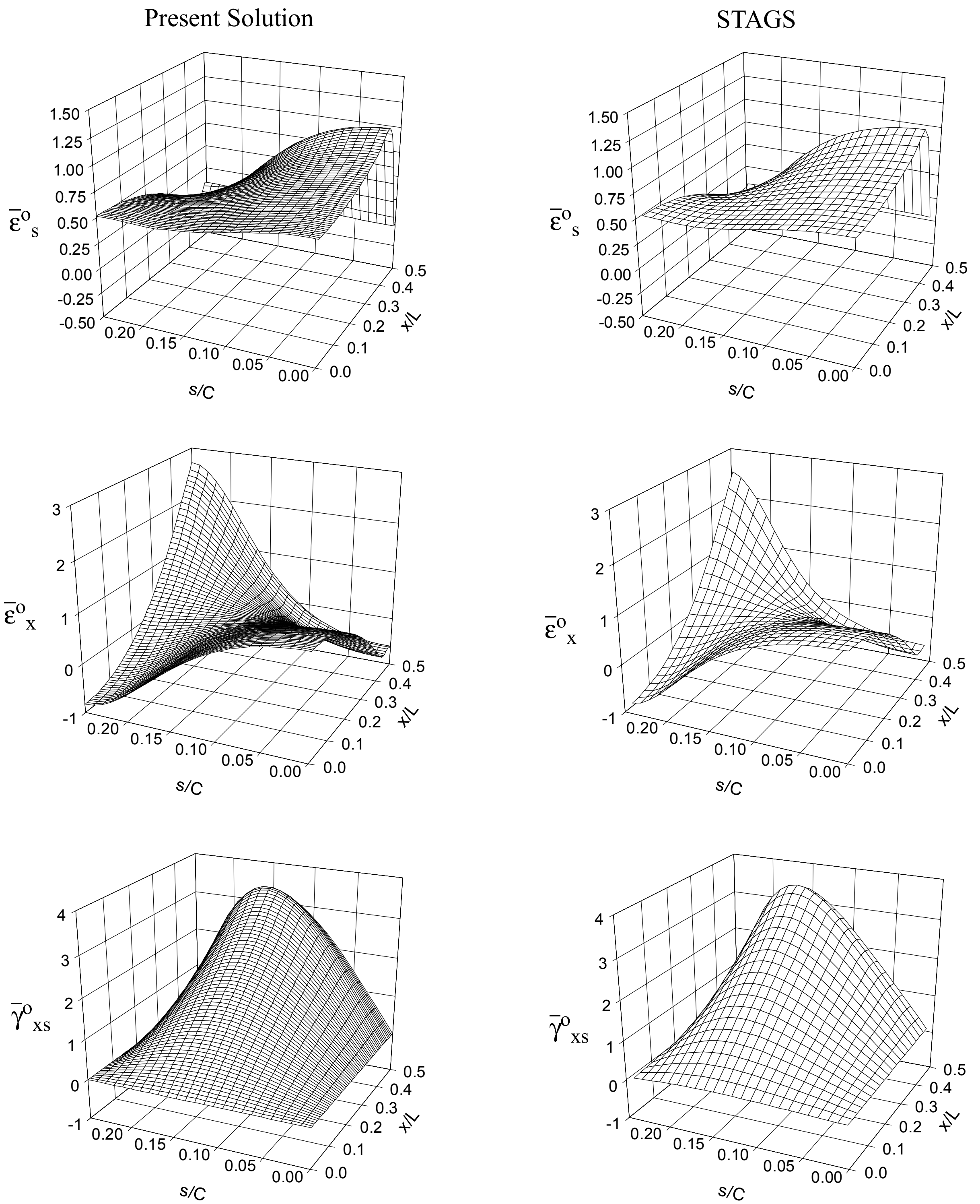

Figure A-14 Comparison between present solution and STAGS for an circumferentially-stiff elliptical cylinder, e=0.7, p_o=100 psi: reference surface strains

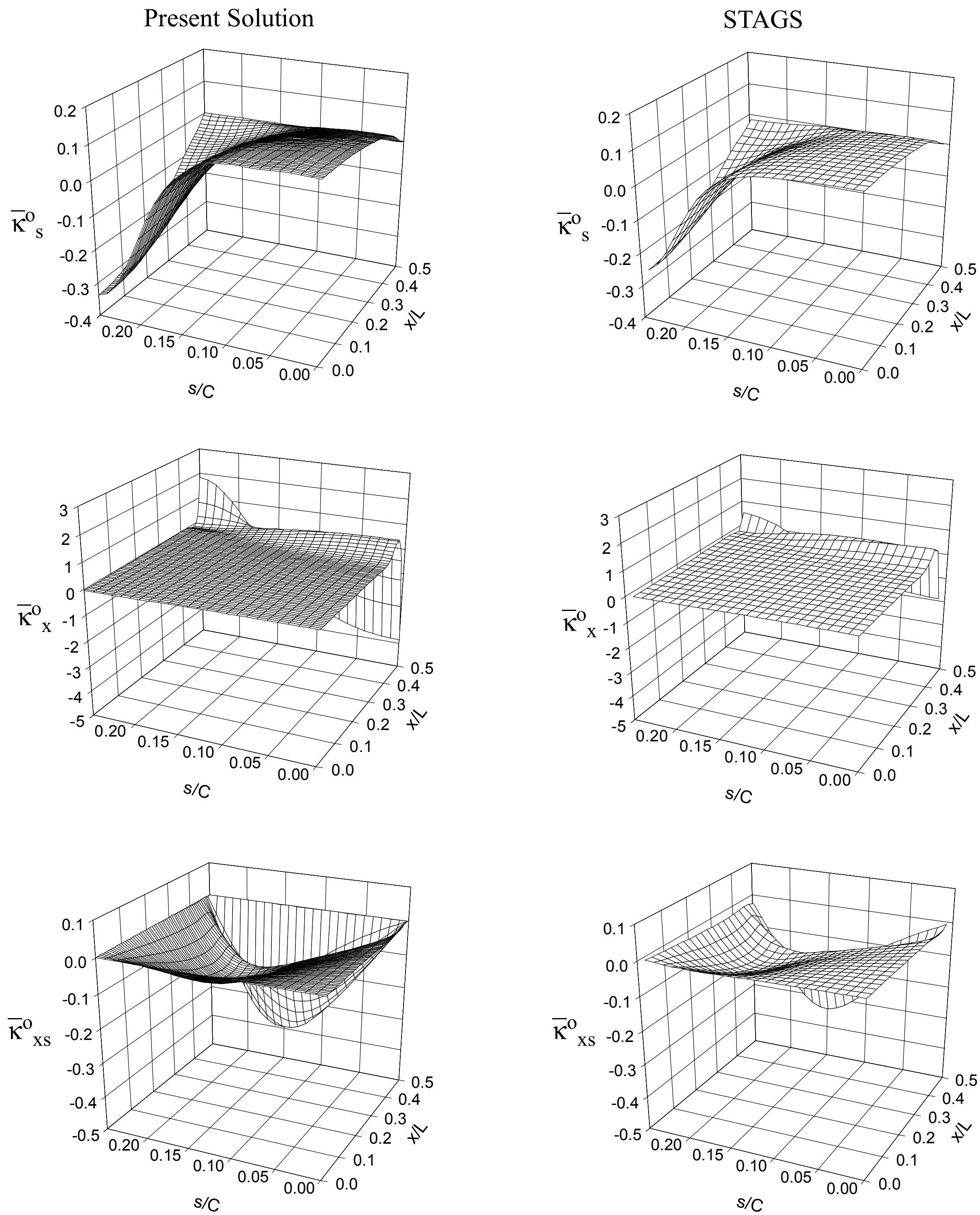

Figure A-15 Comparison between present solution and STAGS for an circumferentially-stiff elliptical cylinder, e=0.7, p_o=100 psi: reference surface curvatures

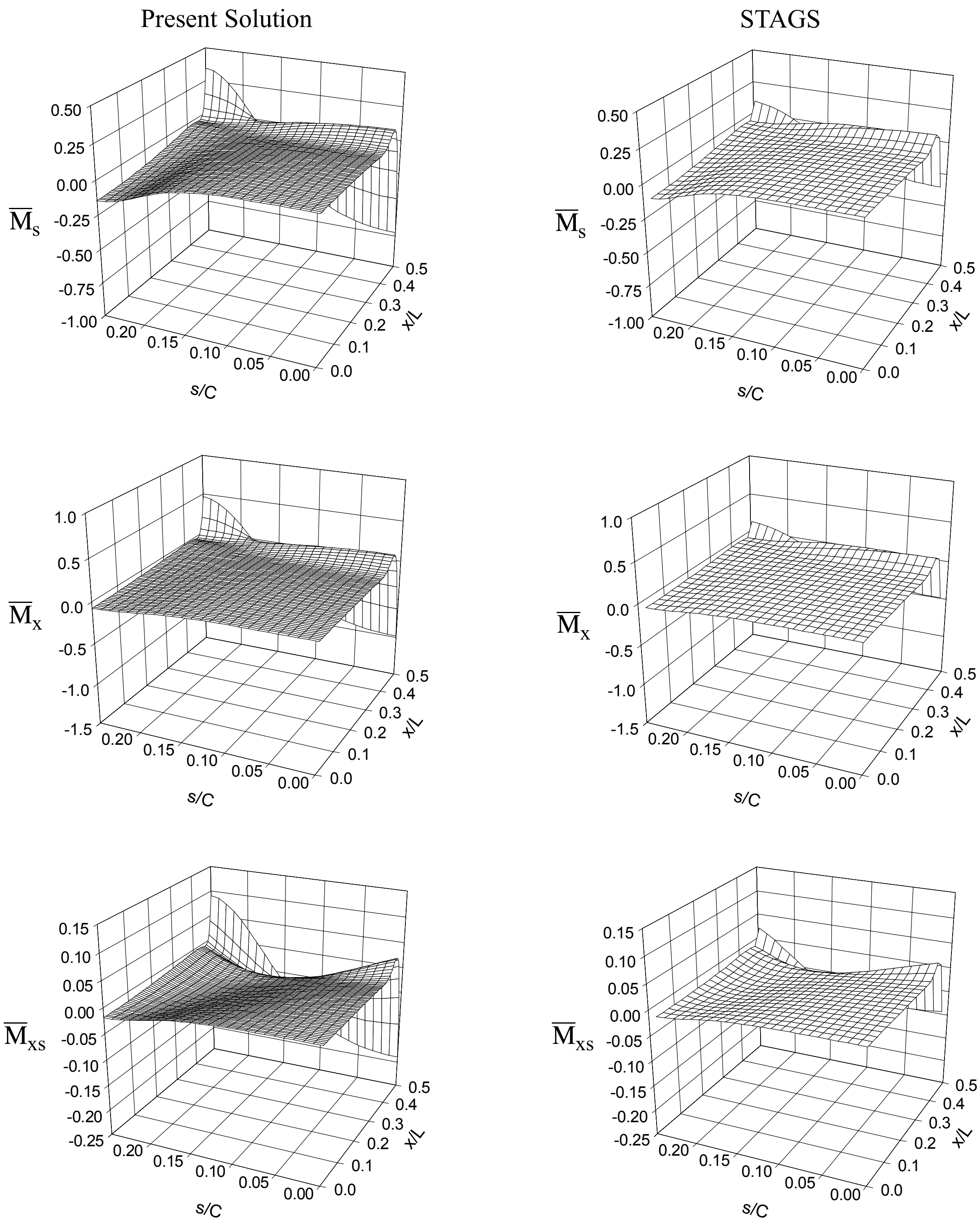

Figure A-16 Comparison between present solution and STAGS for an circumferentially-stiff elliptical cylinder, e=0.7, p_o=100 psi: moment resultants

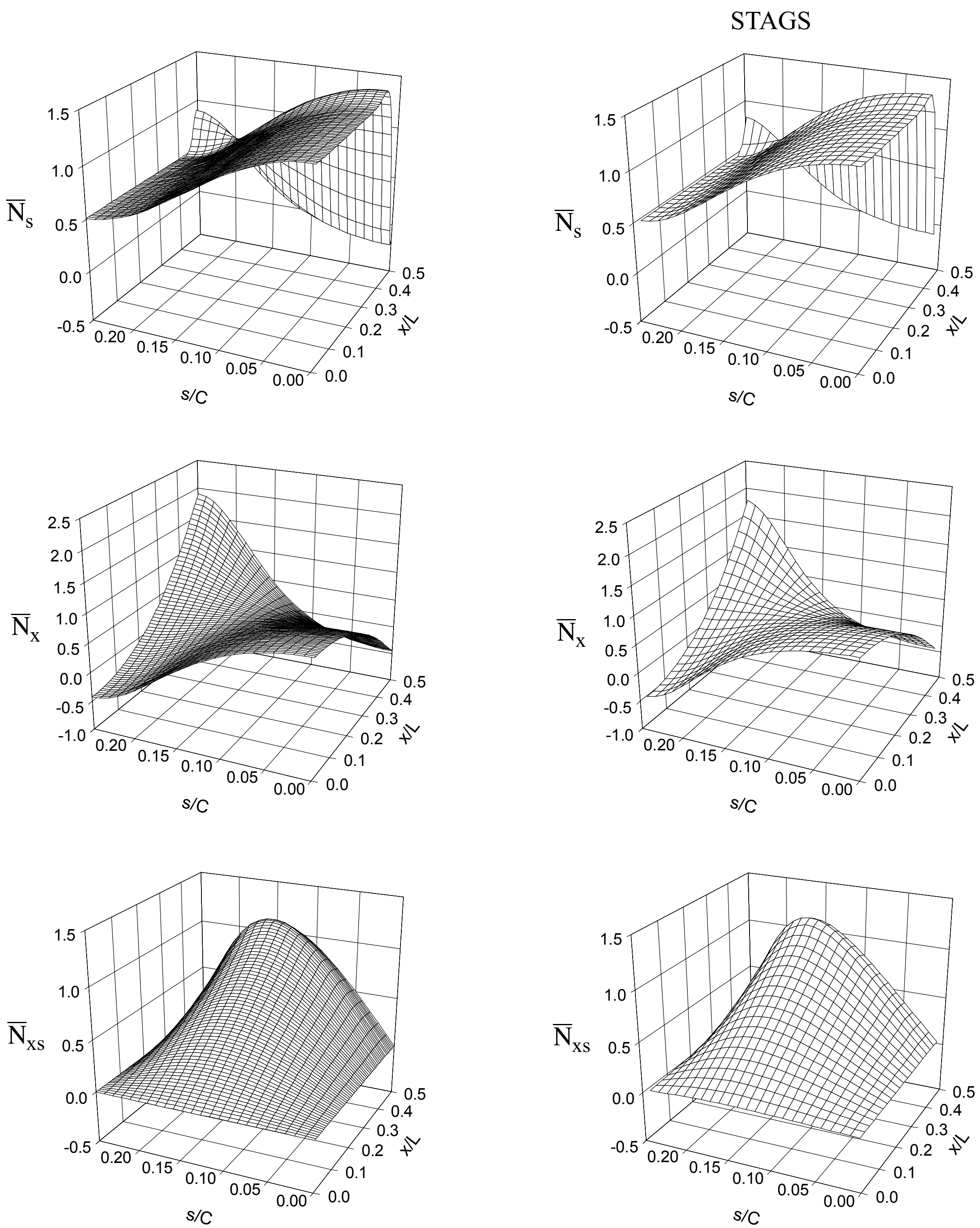

Figure A-17 Comparison between present solution and STAGS for an circumferentially-stiff elliptical cylinder, e=0.7, p_o=100 psi: force resultants

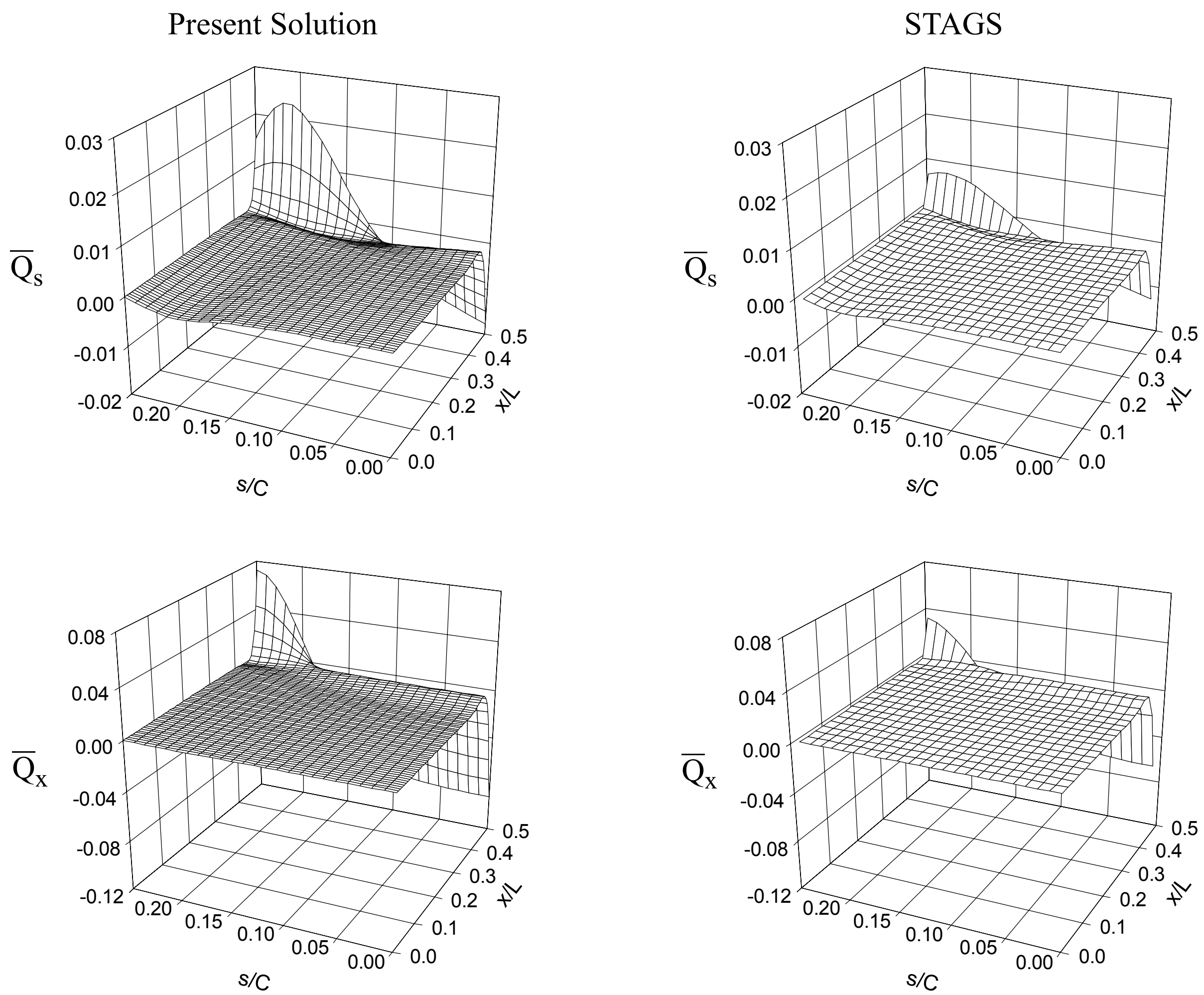

Figure A-18 Comparison between present solution and STAGS for an circumferentially-stiff elliptical cylinder, e=0.7, p_o=100 psi: transverse shear force resultants